INVITED REVIEW

Small animal models of heart failure

Christian Riehle and Johann Bauersachs*

Department of Cardiology and Angiology, Hannover Medical School, Carl-Neuberg-Str. 1, 30625 Hannover, Germany

Abstract   Heart disease is a major cause of death worldwide with increasing prevalence, which urges the development of new therapeutic strategies. Over the last few decades, numerous small animal models have been generated to mimic various pathomechanisms contributing to heart failure (HF). Despite some limitations, these animal models have greatly advanced our understanding of the pathogenesis of the different aetiologies of HF and paved the way to understanding the underlying mechanisms and development of successful treatments. These models utilize surgical techniques, genetic modifications, and pharmacological approaches. The present review discusses the strengths and limitations of commonly used small animal HF models, which continue to provide crucial insight and facilitate the development of new treatment strategies for patients with HF.

Keywords   Animal models • Rodents • Heart failure • HFpEF • HFrEF

1. Introduction

Heart failure (HF) is the leading cause of death worldwide. The mortality rate of HF is high, with about 50% of patients dying within 5 years after the initial diagnosis, which exceeds most types of cancer (www.who.int). Furthermore, the prevalence of HF in industrialized nations is increasing, which results in an enormous economic burden. The increase is attributable, at least in part, to the improved treatment following acute myocardial infarction (MI), which has decreased the mortality rate, but not morbidity, and is based on the number of surviving patients. Additional factors comprise an increased prevalence of comorbidities, which predispose and accelerate the development of HF. Therefore, there is an urgent need to modify these risk factors and to develop new therapeutic strategies for HF patients.

Based on left ventricular (LV) ejection fraction (LVEF), HF can be categorized as *heart failure with preserved ejection fraction* (HFpEF; LVEF ≥50%), *heart failure with mid-range ejection fraction* (HFmrEF; LVEF 40–49%), or *heart failure with reduced ejection fraction* (HFrEF; LVEF < 40%).[1] About 50% of HF patients are afflicted with HFpEF and exhibit HF symptoms, which include exercise intolerance, congestion, and oedema that are associated with cardiac hypertrophy, increased fibrosis, and decreased capillary content. Common risk factors for the development of HFpEF include arterial hypertension, obesity, diabetes mellitus, atrial fibrillation, and renal dysfunction (*Figure 1*). This implies that impaired cardiac compliance and contractile dysfunction found in HFpEF can be triggered by associated comorbidities. Importantly, the postulation that

diastolic dysfunction is equivalent to HFpEF is an oversimplification and only partially correct. This emanates from the observation that diastolic dysfunction has also been detected in normal subjects without clinical HFpEF symptoms.[2] In contrast, HFrEF is typically associated with loss of cardiomyocytes, which can be a consequence of myocardial damage of different aetiologies (*Figure 1*) and may increase wall stress, as reflected by higher levels of natriuretic peptides compared to HFpEF.[2]

Small animal models, including mice, rats, and guinea pigs,[3] continue to improve our understanding of the various aspects and aetiologies of HF and help to develop novel treatment strategies. Mice and rats are the most commonly used animal models and share a high degree of homology to the human genome, with ∼30 000 protein-coding genes each. Major advantages of rodent models include relatively short breeding cycles and low housing costs. Numerous small animal models have been generated as tools to decipher HF aetiologies and develop new HF treatment strategies. These models typically utilize genetic modifications, pharmacological and surgical approaches, which can also be combined. The pathogenesis of HFpEF and HFrEF is multifactorial. Thus, it is often impossible to discern the underlying mechanisms, which can be overlapping and interconnected. This provides a challenge to investigate co-existing risk factors for HF development in a single model organism,[4,5] especially in models of diabetic cardiomyopathy and HFpEF,[6] necessitating the thoughtful selection of the best animal model for a given hypothesis. However, small animal HF models enable the study of specific risk factors without the confounding effect of comorbidities. Over the last few decades, numerous small animal models have greatly advanced our

* Corresponding author. Tel: +49 511 532 3841; fax: +49 511 532 5412, E-mail: bauersachs.johann@mh-hannover.de
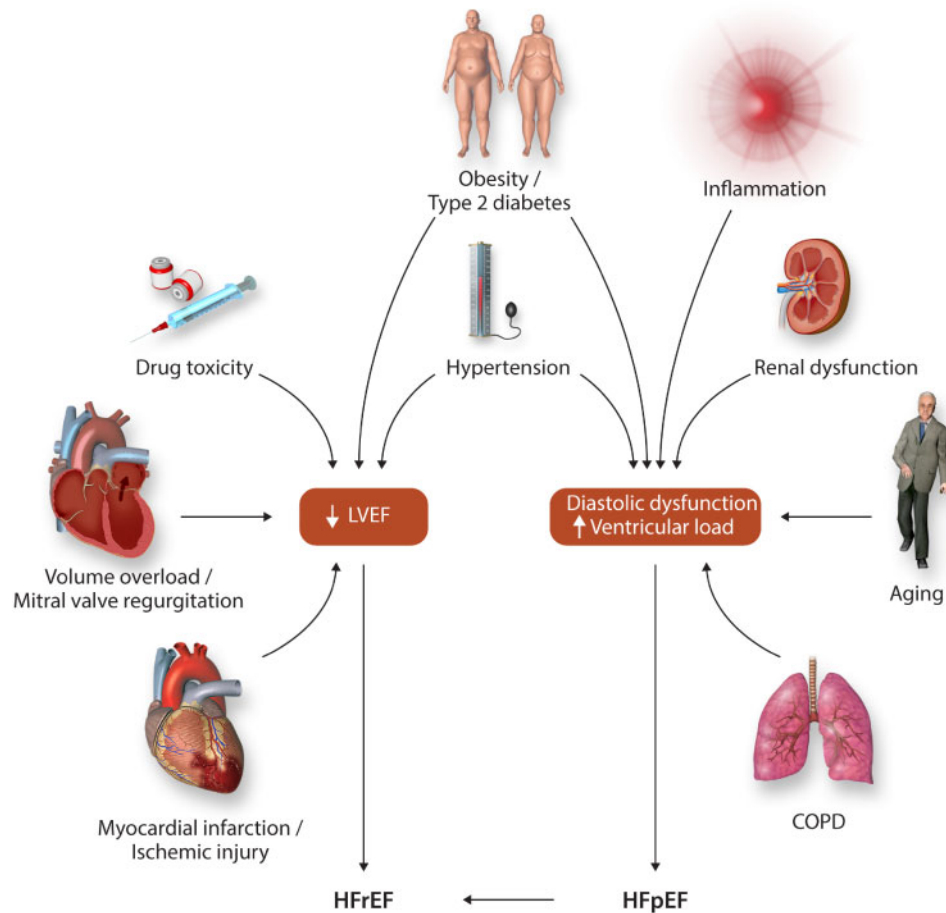
Figure 1 Schematic depicting selected risk factors for the development of heart failure with reduced ejection fraction (HFrEF) and heart failure with preserved ejection fraction (HFpEF). Note that some risk factors increase the risk of both HFrEF and HFpEF, and HFpEF may precede the later onset of HFrEF. COPD, chronic obstructive pulmonary disease; LVEF, left ventricular ejection fraction.

understanding of the pathogenesis of HFrEF and HFpEF, many of which will be highlighted in this article and are summarized in *Table 1*.

2. Small animal models of HFrEF

The following sections discuss rodent models, which typically provoke HFrEF (*Figure 2*). It is important to note that some of these models induce HFpEF, which precedes the later onset of systolic dysfunction and HFrEF.

2.1 Surgical models

2.1.1 LV pressure overload

Chronic LV pressure overload causes HF in mice[7–16] and rats,[7,17,18] which is accomplished by various surgical approaches to mimic the adaptations associated with hypertension and aortic valve stenosis in patients. Transverse aortic constriction (TAC) in mice was first described by Rockman *et al.*[15] and has been subsequently used as a method for LV pressure overload by numerous laboratories. TAC increases LV afterload, which results in concentric cardiac hypertrophy and, ultimately, HFrEF. Several surgical techniques for TAC have been developed, including minimally invasive approaches by a small incision in the proximal

sternum[7,9,10,14] and placement of surgical clips or sutures to impede blood flow across the aortic arch. Recently, a novel method using o-rings with fixed inner diameters has been described, which are placed around the ascending aorta in mice.[83] Measurement of the peak flow velocity difference of the right relative to the left carotid artery enables the quantification of the pressure gradient post-surgery.[7] Important parameters for the hypertrophic response and progression of HF include sex, weight, age, and the genetic background of the species used. Mice with the C57BL/6J genetic background develop HF more rapidly post-TAC compared to the 129S1/SvlmJ strain[11] and have similar gene expression patterns of human dilated cardiomyopathy compared to 129S1/SvlmJ mice.[85] The identified pathways contributing to accelerated HF in C57BL/6J mice include periostin, angiotensin, and IGF1 signalling. Different adaptations for the response to pressure overload have also been reported for the different C57BL/6 substrains, i.e. C57BL/6NCrl (maintained by the Charles River Laboratories), C57BL/6NTac (maintained by the Taconic Laboratories), and C57BL/6J (maintained by the Jackson Laboratory).[84,86] C57BL/6J mice have a mutation in the *nicotinamide nucleotide transhydrogenase (Nnt)* gene, which regenerates NADPH from NADH. This mutation protects C57BL/6J mice from oxidative stress and HF post-TAC compared to the inbred C57BL/6N strain.[84]

Table 1 Characteristics of selected small animal models of heart failure

Model	HF stimulus	Advantage	Limitation	Species	Selected references
Surgical					
LV pressure overload	TAC	Reliable model to induce cardiac hypertrophy and HF.	The acute increase in afterload does not reflect the gradual progression of arterial hypertension and aortic valve stenosis in patients.	Mouse / Rat	7–16 / 7,17,18
	Ascending aortic constriction	Gradual onset of pressure overload, which mimics the gradual progression of arterial hypertension in patients.	Limited relevance to human disease as pressure overload is induced in young animals, whereas arterial hypertension is primarily observed in elderly patients.	Rat	19,20
Temporary LV pressure overload	TAC + removal of the stenosis	Reliable model of cardiac hypertrophy followed by removal of stressor to study reverse cardiac remodelling.	Two surgeries required. Technically challenging technique to remove suture or clip.	Mouse	21–25
MI	LAD ligation	Reliable model to induce tissue damage and HF.	Model does not reflect the clinical setting with reperfusion of the occluded vessel during coronary angiography performed after an acute MI.	Mouse / Rat	26–33 / 34–40
Ischaemia/reperfusion injury	Temporary LAD ligation	Close to clinical scenario with reperfusion of the occluded vessel during coronary angiography performed after an acute MI.	Surgery is more time consuming and more complex than placement of permanent LAD ligation.	Mouse / Rat	41–44 / 44,45
MI (neonatal)	LAD ligation	Identification and characterization of pathways involved in cardiac regeneration.	Limited relevance to human disease. MI and coronary artery disease primarily occur in elderly patients.	Mouse	46
Pressure overload + MI	TAC + LAD ligation	Model mimics the relevant co-morbidities of arterial hypertension and ischaemic heart disease. Gradual and predictable progression of HF.	The acute increase in afterload does not reflect the gradual progression of arterial hypertension in patients.	Mouse	47
	Ascending aortic constriction + LAD ligation	Same as for mouse model of TAC + LAD ligation.	Same as for mouse model of TAC + LAD ligation.	Rat	48
	Abdominal aortic constriction + LAD ligation	Same as for mouse model of TAC + LAD ligation.	Same as for mouse model of TAC + LAD ligation.	Rat	49
Pulmonary hypertension	Pulmonary artery constriction	Model mimics characteristics of RV HF, including increased liver weight and peripheral oedema.	The acute increase in afterload does not reflect the gradual progression of pulmonary hypertension in patients.	Mouse / Rat	50–52 / 53
Volume overload	Aorto-caval fistula (shunt)	Model of chronic volume overload as observed in patients with mitral valve regurgitation. Reproducible model of volume overload-induced HF.	The acute increase in volume overload does not reflect the gradual progression of mitral valve regurgitation in patients. Shunt creates an artificial mix of arterial with venous blood.	Mouse / Rat	12 / 54,55

Continued

Table 1 Continued

| Model	HF stimulus	Advantage	Limitation	Species	Selected references
Drug induced					
Toxic cardiomyopathy	Doxorubicin	Potent stimulus to induce dilated cardiomyopathy.	Systemic toxic effects, especially on bone marrow cells, and gastrointestinal system.	Mouse	56–59
				Rat	60
	Isoproterenol	Potent stimulus to induce cardiac hypertrophy.	Chronic activation of adrenergic signalling is only one contributing factor to the development of HF in patients.	Mouse	8,61
		Drug is easy to administer (i.p. injection or osmotic mini pump).		Rat	62
	Monocrotaline	Model of predominantly RV hypertrophy and RV failure.	Toxicity on other organ systems, i.e. pulmonary and kidney injury.	Rat	63,64
	Homocysteine	Potential clinical relevance; hyperhomo-cysteinaemia is a risk factor for HF.	Hyperhomocysteinaemia represents only one aspect in the development of HF in humans, which is conversely discussed.	Rat	65–67
			Non-specific side effects and toxicity on other organ systems, especially vasculature.		
	Ethanol		Non-specific side effects and toxicity on other organ systems, especially liver.	Rat	68
Hypertension					
Angiotensin II infusion	Chronic stimulation of angiotensin II Type 1 receptor (AT1R) signalling	Reliable model of cardiac hypertrophy.	Unspecific side effects on organ systems, especially kidney.	Mouse	69
		Technically easy surgery to implant osmotic minipumps.		Rat	70
Dahl salt-sensitive rat	Inbred strain of Sprague-Dawley rats, which are susceptible to hypertension following a high-salt diet	Induction of hypertension and HF by high-salt diet feeding without additional surgery.	High housing costs based on the slow progression of hypertension and HF.	Rat	71,72
		Slow progression of hypertension and HF development as observed in patients.			
Spontaneously hypertensive rat (SHR)	Inbred strain of Wistar-Kyoto rats with hypertension	Slow progression of hypertension and HF development as observed in patients.	High housing costs based on the slow progression of hypertension and HF.	Rat	73
T1D					
Akita (Ins2^Akita+/−)	Pancreatic β-cell failure based on mutation in the Insulin2 gene	Robust model for T1D.	High housing costs based on the time-dependent progression of the phenotype.	Mouse	74–76
High-dose STZ	Pancreatic β-cell toxin	Robust model for T1D.	Does not capture the autoimmune contribution to the development of T1D in patients.	Mouse/rat	6

Continued

Table 1 Continued

Model	HF stimulus	Advantage	Limitation	Species	Selected references
Metabolic syndrome/ T2D					
ob/ob	Hyperphagia based on leptin deficiency	Robust phenotype of obesity and T2D.	High housing costs based on the time-dependent progression of the phenotype. Potentially confounding effects of altered leptin-mediated signalling.	Mouse	77,78
db/db	Hyperphagia based on leptin resistance	Robust phenotype of obesity and T2D.	High housing costs based on the time-dependent progression of the phenotype. Potentially confounding effects of altered leptin-mediated signalling.	Mouse	79,80
ZF/ZDF rats	Hyperphagia based on leptin resistance	Model of metabolic syndrome with increased levels of circulating lipids and cholesterol.	High housing costs based on the time-dependent progression of the phenotype. Potentially confounding effects of altered leptin-mediated signalling.	Rat	81,82
High-caloric diet (± low-dose STZ)	High caloric intake (± pancreatic β-cell toxin)	Additional low-dose STZ treatment mimics β-cell failure and late stage T2D.	High housing costs based on the time-dependent progression of the phenotype. Additional low-dose STZ treatment mimics mixture of T1D and T2D.	Rat/mouse	6

Note that housing costs for mice are typically lower than for rats. Another advantage of mouse models is the availability of numerous transgenic strains available. General advantages of rat models are that surgical techniques are easier to perform than in mice.
HF, heart failure; i.p. intraperitoneal; LAD, left anterior descending artery; LV, left ventricular; MI, myocardial infarction; RV, right ventricular; STZ, streptozotocin; T1D, Type 1 diabetes; T2D, Type 2 diabetes; TAC, transverse aortic constriction; ZDF, Zucker diabetic fatty; ZF, Zucker fatty.
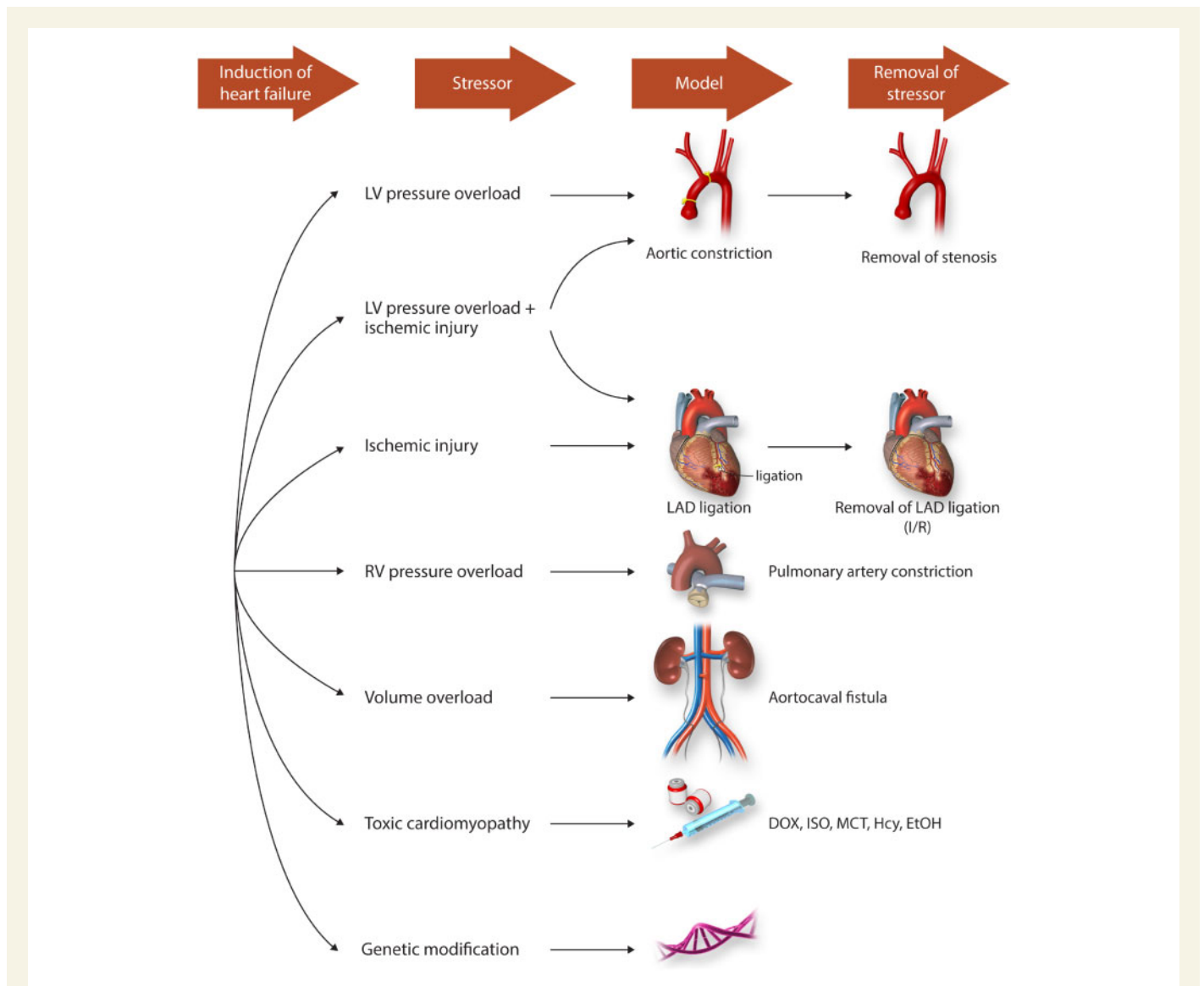
Figure 2 Schematic depicting selected stressors to induce heart failure with reduced ejection fraction (HFrEF) in small animal models. Note that these models may also induce heart failure with preserved ejection fraction (HFpEF), which precedes the later onset of HFrEF. Additional animal models with temporary exposure to drugs and temporary genetic gain-of-function or loss-of-function modifications have been developed. DOX, doxorubicin; EtOH, ethanol; Hcy, homocysteine; I/R, ischaemia/reperfusion injury; ISO, isoproterenol; LAD, left anterior descending artery; LV, left ventriclular; MCT, monocrotaline; RV, right ventriclular.

One important limitation of TAC is the immediate onset of pressure overload, which is in contrast to the slow progression of hypertension and aortic valve stenosis in patients. To overcome this potential drawback, constriction of the ascending aorta has been performed in 3- to 4-week-old rats. In this model, LV hypertrophy is observed by 6 weeks and overt HF by 18 weeks post-surgery.[19,20] Aortic constriction in rats has also been performed around the abdominal aorta both in the infrarenal and suprarenal position, the latter of which induces renal hypoperfusion, hypertension, and LV hypertrophy. Abdominal aortic constriction typically contributes to a slower progression of the HF phenotype.[87] Recently, additional models have been developed that facilitate the study of reverse cardiac remodelling. The models described use different surgical approaches to remove the TAC stenosis and subsequently decrease cardiac workload.[21–25]

2.1.2 Ischaemic injury

Coronary artery ligation is a commonly used, small animal HF model[88] that was initially established by Pfeffer et al.[34] in rats and has been subsequently used by numerous groups.[35–38] The Pfeffer group performed groundbreaking studies and demonstrated that infarct size, post-MI LV chamber dilatation and LV function are correlated. They subsequently showed that treatment with the angiotensin-converting enzyme (ACE) inhibitor captopril improves contractile function and survival following MI in rats.[39,40] The impact of ACE inhibition was subsequently tested in large clinical trials in patients post-MI, which improved contractile function and survival.[89] These studies established pharmacological ACE inhibition for patients with MI, which is now a commonly used, standard treatment. Coronary artery ligation has also been performed in mouse models.[26–33] Ligation of the left anterior descending (LAD) artery

typically results in HF 4 weeks post-surgery and strongly depends on the genetic background of the mice used.[32] One potential limitation of these animal models with permanent coronary artery occlusion is the differences in their observed phenotypes relative to those observed in patients; atherosclerosis of the coronary arteries in patients results in ischaemic heart disease that slowly progresses and coronary artery blood flow can eventually be re-established during coronary angiography performed after an acute MI. To overcome this limitation, ischaemia/reperfusion (I/R) models have been established, which facilitate the investigation of molecular mechanisms and tissue damage following temporary LAD occlusion.[41–45,90] The I/R model typically exhibits less tissue damage compared to permanent LAD occlusion. Importantly, ischaemic injury is typically induced in young rodent models. This is in contrast to the patient population, in which elderly and multimorbid patients exhibit the greatest risk of coronary artery disease and acute MI.

MI has also been induced in neonatal mice to identify and characterize pathways that are involved in cardiac regeneration. Ischaemic injury in neonatal mice is provoked by LAD ligation and complete recovery is observed by 3 weeks of age. The regenerative potential decreases as the mice age and the abundance of proliferating cardiomyocytes diminishes.[46] Similar to TAC, the adaptations post-MI have been compared across the most commonly used mouse strains and are dependent on genetic background. While infarct rupture was most frequently observed in 129S6 mice, cardiac dilatation was most prominent in Swiss mice.[32] Therefore, the genetic background should be an important consideration in study designs.

2.1.3 Combined LV pressure overload/ischaemic injury

To explore the coexistence of clinically relevant morbidities of arterial hypertension and coronary artery disease present in patients, recent surgical HF models combine the techniques of TAC surgery and LAD ligation. This combined surgical approach was first described in rats[48] and has since been modified for mouse models.[47] Various models have been published with different locations for the placement of the aortic stenosis, all of which exhibit adverse LV remodelling and rapid HF progression.[49] Recently, a mouse model with combined MI and temporary TAC was developed,[91] which has enabled the elucidation of the impact of mechanical unloading following ischaemic injury.

2.1.4 Right ventricular pressure overload

Similarly to TAC surgery, which increases LV afterload, pulmonary artery banding increases right ventricular (RV) afterload, and mimics pulmonary hypertension in mice[50–52] and rats.[53] Pulmonary artery banding results in RV hypertrophy and pathological remodelling.[50] As reported for TAC, the severity of the pulmonary artery stenosis correlates with the progression of contractile dysfunction and mortality.[51] Notably, the acute increase in RV afterload does not reflect the gradual progression of pulmonary hypertension in patients.

2.1.5 Volume overload

Chronic volume overload in small animal models reproduces the pathologies observed in patients with mitral valve regurgitation, which typically increase diastolic wall stress and cause eccentric cardiac hypertrophy.[12] Cardiac volume overload is accomplished in rodents by creating a surgical aorto-caval shunt and has been reported for rats[54,55] and mice.[12] Volume overload in rats initially decreases LV function. The subsequent compensatory hypertrophy normalizes contractile function at one month post-surgery,[54] with the time course of HF development strongly

depending on the shunt volume and being less predictable compared to TAC models. The shunt creates an artificial mix of arterial with venous blood, which is in contrast to the clinical setting in patients with mitral valve regurgitation. Volume overload in mice causes minimal apoptosis in the absence of pathological remodelling, which is in contrast to the increased afterload following TAC surgery. This indicates that increased preload, i.e. aorto-caval shunt, and increased afterload, i.e. TAC, contribute to different morphological phenotypes, which is important for the design of future HF therapies.

2.2 Toxic cardiomyopathy

The anthracycline compound Doxorubicin (DOX) is a standard anti-cancer therapeutic agent. DOX causes dilated cardiomyopathy in a dose-dependent manner[92] that is typically irreversible and progressive. DOX has been administered to numerous small animal models[56–60] and promotes the formation of free radicals and mitochondrial dysfunction.[93,94] Juvenile DOX exposure in mice results in no immediate contractile dysfunction, however, impairs the ability to adapt to angiotensin II-induced hypertension later in life, which is restored by co-treatment with resveratrol.[95] Notably, cancer cachexia increases the risk of HF and decreases systemic insulin levels. Chronic insulin supplementation decreases glucose usage by the tumour, normalizes cancer-mediated impairment in cardiac Akt signalling and attenuates contractile dysfunction.[96] Conversely, HF following MI increases tumour growth as reported for APC[Min] mice that have a mutation in the tumour suppressor gene *Adenomatosis polyposis coli (Apc)* and are prone to multiple intestinal neoplasia (Min) and cancer development.[97]

Chronic stimulation of G-protein-coupled ß-adrenergic receptor signalling with isoproterenol provokes cardiomyocyte hypertrophy and fibrosis in mice[8,61] and rats,[62] which is similar to the progressive HF development in mice with cardiac-specific overexpression of β_1-adrenergic receptors.[98] The mechanisms responsible include an imbalance between the increased energy demand, which is based on the hypercontractility of the myocardium relative to the oxygen and nutrients provided.

Monocrotaline (MCT) is a pyrrolizidine alkaloid obtained from the plant species *Crotalaria spectabilis*, which induces pulmonary hypertension and RV hypertrophy. MCT is converted in the liver to MCT pyrrole and circulates to the lung parenchyma to increase capillary permeability and to trigger interstitial oedema and smooth muscle hypertrophy.[99] These alterations increase pulmonary vascular resistance, RV pressure overload, and RV failure. MCT has been used in rats[63,64] and larger animal models. Importantly, non-specific side effects for MCT have been reported, such as lung and kidney injury,[64,99] which are important to consider when designing future studies.

As previously reviewed, high circulating homocysteine levels are a risk factor for the future onset of HF.[100] Similarly, dietary supplementation with homocysteine increases inflammation, collagen remodelling, and oxidative stress,[65,66,100] and provokes contractile dysfunction in both normotensive and spontaneously hypertensive rats.[65–67] Chronic ethanol ingestion contributes to dilated cardiomyopathy in both rodent models and humans.[101] The underlying mechanisms comprise decreased myocardial contractility as a consequence of altered myofibrillar Mg^{2+}-ATPase activity and cardiomyocyte loss.[68]

2.3 Genetically engineered models

Numerous transgenic animal models of HF have been generated to investigate the impact of genetic modifications, typically gain-of-function or

loss-of-function modifications, on cellular and molecular processes contributing to clinically relevant phenotypes.[102,103] The complex topic of genetic modification for the generation of transgenic mouse models has been reviewed in detail.[104] Transgenic mice with whole body gene deletions have been developed (constitutive knockouts). Confounders that emanate from the deletion of a gene throughout the entire organism resulted in the development of tools to generate conditional knockouts with spatial and temporal gene deletion. Gene deletion can be facilitated by Cre/loxP- or Flippase/FRT-mediated recombination, and tissue-specific Cre and Flippase recombination are achieved by the use of a specific promoter (e.g. *myosin heavy chain 6, Myh6*). Recently, engineered nucleases have been developed to modulate DNA sequences and to generate transgenic mice. The nucleases used for genome editing include transcription activator-like effector nuclease (TALEN), zinc-finger nuclease (ZFN), and clustered regularly interspaced short palindromic repeat (CRISPR)/-associated protein 9 (Cas9). Compared to other nucleases, the CRISPR/Cas9 system is more efficient and the design of constructs easier to perform.[104] Important limitations of the CRISPR/Cas9 system are non-specific off-target effects, which can affect the phenotype of the model generated and necessitate whole-genome sequencing of the generated mouse model. Genetic modification can also be facilitated by adeno-associated virus (AAV)-mediated delivery of DNA constructs, which can be performed by the use of a combination of specific viral serotypes and promotors (e.g. AAV9 and *Myh6*).[105] Compared to the generation of transgenic animals, virus-mediated approaches are usually more time- and cost-efficient. Potential drawbacks include side effects in other tissues following systemic injection and badge-to-badge variability of the virus construct.

3. Small animal models of HFpEF

In the following sections, we will discuss the most common models to investigate classical risk factors for the development of HFpEF, which include hypertension, obesity, diabetes mellitus, and aging. Importantly, systolic contractile dysfunction may also be present in these models, which additionally enables their use as HFrEF models. Additional risk factors for the development of HFpEF in humans include renal dysfunction, chronic obstructive pulmonary disease (COPD) and atrial fibrillation, which have not been studied in detail in small animal models.

3.1 Hypertension

The Dahl salt-sensitive rat, which was generated by inbreeding Sprague-Dawley rats,[71] is one of the most commonly used HFpEF models. When fed with a high-salt diet containing 8% NaCl, this model rapidly develops hypertension, diastolic dysfunction, and HFrEF.[72] Spontaneously hypertensive rat is an inbred strain of Wistar-Kyoto rats with hypertension.[73] Chronic infusion with angiotensin II causes hypertension and cardiomyocyte hypertrophy in mice and rats.[69,70] Major advantages of these models are the slow progression of hypertension and HF, which is also observed in patients with hypertension and is in contrast to the immediate increase in LV workload following TAC surgery.

3.2 Obesity and diabetes mellitus

Numerous small animal models have been generated to investigate the impact of Type 1 (T1D) and Type 2 diabetes (T2D) on the heart.[6] A commonly used model for T1D is the Akita mouse (*Ins2*^Akita+/-^), which exhibits a mutation in the *Insulin2* encoding gene. This results in misfolding of the insulin protein, endoplasmic reticulum stress, and β-cell

failure.[74] Hearts from Akita mice show increased inflammation[75] and diastolic dysfunction in the presence of normal systolic function.[76]

The glucosamine-nitrosourea streptozotocin (STZ) is toxic to pancreatic β-cells and has been used to study both T1D and T2D. Because of its structural similarity to glucose, STZ enters pancreatic β-cells via the glucose transporter 2 (GLUT2), causing cellular damage, and impairing insulin production. The STZ-mediated effects on β-cell destruction and hyperglycaemia are dose-dependent. High-dose STZ treatment induces T1D in rodents. In contrast, low-dose STZ protocols have been used to overcome the low penetrance of some high-calorie dietary regimens and to mimic β-cell failure and late stage T2D. Therefore, low-dose STZ treatment has been added to the high-fat diet (HFD) protocols.[6]

Ob/ob[77] and db/db[79] mice are commonly used models of obesity and T2D that are based on leptin resistance or deficiency, respectively. Diastolic dysfunction has been reported for both models.[78,80] Additional models for T2D and insulin resistance include Zucker fatty (ZF) rats, which express non-functional leptin receptors[81] and Zucker diabetic fatty rats, which are an inbred strain of ZF rats with high serum glucose levels.[82]

Numerous dietary treatment regimens are used to induce insulin resistance and T2D in rodents. HFD chow usually contains a total fat content of up to 60%. Rodent 'Western' diets typically contain a high content in fat and sucrose, which makes them a useful tool to study pathologies that have been described by the 'Western' dietary pattern in humans.[106] Depending on the total fat content and duration these dietary treatments may induce contractile dysfunction in rodents. The proposed mechanisms have been recently discussed in detail.[6,102]

3.3 Aging

HFpEF is primarily found in elderly patients. Senescence-accelerated prone (SAMP) mice have been generated by selective inbreeding of AKR/mice with inherited senescence[107] and have been subsequently used to study various effects of aging. SAMP mice develop age-dependent diastolic dysfunction, adverse remodelling, endothelial cell dysfunction, and HFpEF when subjected to a high-salt, HFD. These studies suggest endothelial cell dysfunction as one potential mechanism contributing to the age-dependent increase in HFpEF in patients.[108,109]

4. General advantages and limitations using small animal models

General advantages of small animal models include a lower housing cost compared to large animals, shorter gestation times and reduced costs for pharmacological treatments, which is typically administered proportionally to body weight. The potential increase in sample size improves statistical power. Recent advancements in magnetic resonance imaging, high-resolution transthoracic echocardiography, and micromanometer conductance catheters enable a detailed assessment of contractile function even in small rodents. Major advantages of mouse models compared to rats are the availability of a variety of already existing transgenic strains and readily available tools to generate novel transgenic lines. Therefore, transgenic mouse models also facilitate the investigation of specific genetic modifications in the context of superimposed stressors, for example using a surgical model or dietary treatment. Genetic modifications using viral vectors are typically easier to introduce into the genome of small rodents compared to larger animals. This mainly results from the

amount of virus required for sufficient transduction, which is typically proportional to body weight. Intravenous delivery of AAV9, for example, results in a very low transduction rate of cardiomyocytes in dogs.[110] Based on the technical challenge to transduce myocardial tissue of large animals, surgical and catheter-based approaches have been developed to overcome this limitation. In contrast, AAVs that target the myocardium of small rodents can easily be delivered by intravenous and intraperitoneal injection. Using transgenic gain-of-function models, it is important to consider that high levels of overexpression can cause HF per se, as reported for transgenic overexpression of the biologically inactive green fluorescent protein (GFP).[111]

Despite these advantages, several limitations using small animal models warrant attention. Rodents are typically on the same or very similar genetic background, which does not reflect the genetic heterogeneity of the patient population. Another limitation of small animal models, especially surgical models, is the rapid induction of the stressor, which is in contrast to the typically slow disease progression in patients. HF and coronary artery disease are often associated with atherosclerosis in patients, which is difficult to induce in most small rodent models. Several differences comparing the murine and human heart exist that result from the difference in heart rate. In general, the heart rate and the size of the species are inversely correlated, with about 500–600 beats per minute (b.p.m.) in mice, 350 b.p.m. in rats, 60–80 b.p.m. in humans, 30 b.p.m. in elephants, and 6 b.p.m. in blue whales.[112,113] Human ventricular myocytes predominately express β-myosin heavy chain (MHC). Adult murine cardiomyocytes mainly express α-MHC with rapid ATPase activity, which facilitates a contraction rate of up to ∼600 b.p.m. Action potentials in murine cardiomyocytes exhibit a rapid repolarization phase, lack a prominent plateau phase and have a shorter total duration compared to human cardiomyocytes. This facilitates faster contraction/relaxation compared to larger mammals, which is required to sustain cardiac output (calculation: stroke volume × heart rate) at high heart rates. Based on these contractile kinetics, the ability to increase heart rates in small animal models is impaired relative to humans, which can typically increase by up to approximately three-fold. In contrast, the heart rate of mice can increase by about 30–40% under exercise conditions, which limits cardiac reserve and is an important consideration in the design of exercise studies.

In humans, HF is typically observed in older patients, in contrast to most rodent models, in which HF is commonly induced by various stressors starting at young ages to reduce experimental costs. Depending on the extent and duration of the stressor, rodent models with HFpEF may also develop HFrEF. In contrast, several disease conditions are associated with HFpEF in humans, which typically do not progress to HFrEF, such as hypertensive heart disease.

5. General considerations for the use of small and large animal models

Despite the specific limitations and differences outlined above, myocardial energetics and contraction are overall relatively similar between small rodents and humans. Consequently, numerous proteins share functions across species, which makes small rodent models inevitable tools to rapidly conduct proof-of-principle studies at a large scale and to test for different druggable targets and genetic modifications over a relatively short-time period. However, despite their widespread use and acceptance, studies performed in small rodent models should be interpreted with caution. Different phenotypes for humans with genetic mutations and transgenic mice recapitulating diseases were observed. For example, patients with Duchenne Muscular Dystrophy, which lack the expression of the dystrophin protein, have an average survival rate of about 40 years, with about 10-20% of patients developing HF. In contrast, dystrophin-deficient mice have a normal life span and relatively mild cardiomyopathy (reviewed in Ref.[114]). Another example is the nonsense T116G mutation in the phospholamban (PLB) gene in patients with dilated cardiomyopathy, which results in severe HF. Conversely, PLB deficient-mice exhibit enhanced cardiac contractility and a normal life span.[115] Several drugs have also been tested in small animal models with beneficial effects observed, despite their failure in humans.[116] Examples include the phosphodiesterase (PDE) 5 inhibitor Sildenafil, which attenuated the onset of HF post-TAC in mice[117] but showed no benefit in chronic HF patients in the RELAX trial.[118] Relaxin and the recombinant protein Serelaxin also attenuated adverse remodelling post-MI in mice[119] but showed no beneficial effects in humans with acute HF in the RELAX-AHF-2 trial.[120]

These examples highlight different adaptations of small animal models with genetic modifications and pharmacological treatments compared to patients. As a result, results from small animal models should be validated in large animals prior to Phase I trials in humans. Swine is a prototypical pre-clinical large animal model. Advantages of swine are a similar expression pattern of MHC isoforms and a similar reserve in heart rate and cardiac output compared to humans. Importantly, animal models are typically subjected to an single-drug treatment in the context of a HF stressor and beneficial effects for a specific drug tested might be observed. However, these effects may not be observed in later clinical trials, in which patients typically receive the drug in addition to the well-established standard treatment for chronic HF. This also provides a potential explanation for the successful bench-to-bedside translation of the very early studies performed by the Pfeffer group using ACE inhibitors and the failure of numerous later clinical studies, which showed efficacy in animal models, but not in patients.

6. Summary and conclusion

Small animal models, especially mice and rats, mimic various aspects of the pathogenesis of HF and help to decipher various underlying contributing mechanisms of the disease. Several limitations for small animal studies exist that warrant the interpretation of the results of the studies performed with caution. Despite these specific limitations, small animal models serve as invaluable tools that have greatly advanced our understanding of the pathogenesis of HF. Based on recent advancements in genome editing, numerous novel transgenic models are likely to be generated in the near future. These models will continue to facilitate the identification of new targets and to develop novel treatment strategies for HF patients.

Conflict of interest: none declared.

Funding

References

1. Ponikowski P, Voors AA, Anker SD, Bueno H, Cleland JG, Coats AJ, Falk V, Gonzalez-Juanatey JR, Harjola VP, Jankowska EA, Jessup M, Linde C, Nihoyannopoulos P, Parissis JT, Pieske B, Riley JP, Rosano GM, Ruilope LM, Ruschitzka F, Rutten FH, van der Meer P; Authors/Task Force Members; Document Reviewers. 2016 ESC Guidelines for the diagnosis and treatment of acute and chronic heart failure: the Task Force for the diagnosis and treatment of acute and chronic heart failure of the European Society of Cardiology (ESC). Developed with the special contribution of the Heart Failure Association (HFA) of the ESC. *Eur J Heart Fail* 2016;**18**:891–975.

2. Valero-Munoz M, Backman W, Sam F. Murine models of heart failure with preserved ejection fraction: a "fishing expedition". *JACC Basic Transl Sci* 2017;**2**:770–789.

3. Goh KY, Qu J, Hong H, Liu T, Dell'Italia LJ, Wu Y, O'Rourke B, Zhou L. Impaired mitochondrial network excitability in failing guinea-pig cardiomyocytes. *Cardiovasc Res* 2016;**109**:79–89.

4. Sorop O, Heinonen I, van Kranenburg M, van de Wouw J, de Beer VJ, Nguyen ITN, Octavia Y, van Duin RWB, Stam K, van Geuns RJ, Wielopolski PA, Krestin GP, van den Meiracker AH, Verjans R, van Bilsen M, Danser AHJ, Paulus WJ, Cheng C, Linke WA, Joles JA, Verhaar MC, van der Velden J, Merkus D, Duncker DJ. Multiple common comorbidities produce left ventricular diastolic dysfunction associated with coronary microvascular dysfunction, oxidative stress, and myocardial stiffening. *Cardiovasc Res* 2018;**114**:954–964.

5. O'Gallagher K, Shah AM. Modelling the complexity of heart failure with preserved ejection fraction. *Cardiovasc Res* 2018;**114**:919–921.

6. Riehle C, Bauersachs J. Of mice and men: models and mechanisms of diabetic cardiomyopathy. *Basic Res Cardiol* 2018;**114**:2.

7. Riehle C, Wende AR, Zaha VG, Pires KM, Wayment B, Olsen C, Bugger H, Buchanan J, Wang X, Moreira AB, Doenst T, Medina-Gomez G, Litwin SE, Lelliott CJ, Vidal-Puig A, Abel ED. PGC-1beta deficiency accelerates the transition to heart failure in pressure overload hypertrophy. *Circ Res* 2011;**109**:783–793.

8. Thum T, Gross C, Fiedler J, Fischer T, Kissler S, Bussen M, Galuppo P, Just S, Rottbauer W, Frantz S, Castoldi M, Soutschek J, Koteliansky V, Rosenwald A, Basson MA, Licht JD, Pena JT, Rouhanifard SH, Muckenthaler MU, Tuschl T, Martin GR, Bauersachs J, Engelhardt S. MicroRNA-21 contributes to myocardial disease by stimulating MAP kinase signalling in fibroblasts. *Nature* 2008;**456**:980–984.

9. Hu P, Zhang D, Swenson L, Chakrabarti G, Abel ED, Litwin SE. Minimally invasive aortic banding in mice: effects of altered cardiomyocyte insulin signaling during pressure overload. *Am J Physiol Heart Circ Physiol* 2003;**285**:H1261–H1269.

10. Pereira RO, Wende AR, Crum A, Hunter D, Olsen CD, Rawlings T, Riehle C, Ward WF, Abel ED. Maintaining PGC-1alpha expression following pressure overload-induced cardiac hypertrophy preserves angiogenesis but not contractile or mitochondrial function. *FASEB J* 2014;**28**:3691–3702.

11. Barrick CJ, Rojas M, Schoonhoven R, Smyth SS, Threadgill DW. Cardiac response to pressure overload in 129S1/SvImJ and C57BL/6J mice: temporal- and background-dependent development of concentric left ventricular hypertrophy. *Am J Physiol Heart Circ Physiol* 2007;**292**:H2119–H2130.

12. Toischer K, Rokita AG, Unsold B, Zhu W, Kararigas G, Sossalla S, Reuter SP, Becker A, Teucher N, Seidler T, Grebe C, Preuss L, Gupta SN, Schmidt K, Lehnart SE, Kruger M, Linke WA, Backs J, Regitz-Zagrosek V, Schafer K, Field LJ, Maier LS, Hasenfuss G. Differential cardiac remodeling in preload versus afterload. *Circulation* 2010;**122**:993–1003.

13. Rockman HA, Ross RS, Harris AN, Knowlton KU, Steinhelper ME, Field LJ, Ross J Jr, Chien KR. Segregation of atrial-specific and inducible expression of an atrial natriuretic factor transgene in an in vivo murine model of cardiac hypertrophy. *Proc Natl Acad Sci USA* 1991;**88**:8277–8281.

14. Faerber G, Barreto-Perreia F, Schoepe M, Gilsbach R, Schrepper A, Schwarzer M, Mohr FW, Hein L, Doenst T. Induction of heart failure by minimally invasive aortic constriction in mice: reduced peroxisome proliferator-activated receptor gamma coactivator levels and mitochondrial dysfunction. *J Thorac Cardiovasc Surg* 2011;**141**:492–500.e491.

15. Rockman HA, Wachhorst SP, Mao L, Ross J Jr. ANG II receptor blockade prevents ventricular hypertrophy and ANF gene expression with pressure overload in mice. *Am J Physiol* 1994;**266**:H2468–H2475.

16. Grund A, Szaroszyk M, Döppner JK, Malek Mohammadi M, Kattih B, Korf-Klingebiel M, Gigina A, Scherr M, Kensah G, Jara-Avaca M, Gruh I, Martin U, Wollert KC, Gohla A, Katus HA, Müller OJ, Bauersachs J, Heineke J. A gene therapeutical approach to inhibit calcium and integrin binding protein 1 ameliorates maladaptive remodelling in pressure overload. *Cardiovasc Res* 2019;**115**:71–82.

17. Schwarzer M, Osterholt M, Lunkenbein A, Schrepper A, Amorim P, Doenst T. Mitochondrial reactive oxygen species production and respiratory complex activity in rats with pressure overload-induced heart failure. *J Physiol (Lond)* 2014;**592**:3767–3782.

18. Schwarzer M, Schrepper A, Amorim PA, Osterholt M, Doenst T. Pressure overload differentially affects respiratory capacity in interfibrillar and subsarcolemmal mitochondria. *Am J Physiol Heart Circ Physiol* 2013;**304**:H529–H537.

19. Schunkert H, Dzau VJ, Tang SS, Hirsch AT, Apstein CS, Lorell BH. Increased rat cardiac angiotensin converting enzyme activity and mRNA expression in pressure overload left ventricular hypertrophy. Effects on coronary resistance, contractility, and relaxation. *J Clin Invest* 1990;**86**:1913–1920.

20. Litwin SE, Katz SE, Weinberg EO, Lorell BH, Aurigemma GP, Douglas PS. Serial echocardiographic-Doppler assessment of left ventricular geometry and function in rats with pressure-overload hypertrophy. Chronic angiotensin-converting enzyme inhibition attenuates the transition to heart failure. *Circulation* 1995;**91**:2642–2654.

21. Zhang X, Javan H, Li L, Szucsik A, Zhang R, Deng Y, Selzman CH. A modified murine model for the study of reverse cardiac remodelling. *Exp Clin Cardiol* 2013;**18**:e115–e117.

22. Andersen NM, Stansfield WE, Tang RH, Rojas M, Patterson C, Selzman CH. Recovery from decompensated heart failure is associated with a distinct, phase-dependent gene expression profile. *J Surg Res* 2012;**178**:72–80.

23. Byrne NJ, Levasseur J, Sung MM, Masson G, Boisvenue J, Young ME, Dyck JR. Normalization of cardiac substrate utilization and left ventricular hypertrophy precede functional recovery in heart failure regression. *Cardiovasc Res* 2016;**110**:249–257.

24. Stansfield WE, Rojas M, Corn D, Willis M, Patterson C, Smyth SS, Selzman CH. Characterization of a model to independently study regression of ventricular hypertrophy. *J Surg Res* 2007;**142**:387–393.

25. Hariharan N, Ikeda Y, Hong C, Alcendor RR, Usui S, Gao S, Maejima Y, Sadoshima J. Autophagy plays an essential role in mediating regression of hypertrophy during unloading of the heart. *PLoS One* 2013;**8**:e51632.

26. Fraccarollo D, Berger S, Galuppo P, Kneitz S, Hein L, Schutz G, Frantz S, Ertl G, Bauersachs J. Deletion of cardiomyocyte mineralocorticoid receptor ameliorates adverse remodeling after myocardial infarction. *Circulation* 2011;**123**:400–408.

27. Fraccarollo D, Galuppo P, Sieweke JT, Napp LC, Grobbecker P, Bauersachs J. Efficacy of mineralocorticoid receptor antagonism in the acute myocardial infarction phase: eplerenone versus spironolactone. *ESC Heart Fail* 2015;**2**:150–158.

28. Frantz S, Hofmann U, Fraccarollo D, Schafer A, Kranepuhl S, Hagedorn I, Nieswandt B, Nahrendorf M, Wagner H, Bayer B, Pachel C, Schon MP, Kneitz S, Bobinger T, Weidemann F, Ertl G, Bauersachs J. Monocytes/macrophages prevent healing defects and left ventricular thrombus formation after myocardial infarction. *FASEB J* 2013;**27**:871–881.

29. Galuppo P, Vettorazzi S, Hovelmann J, Scholz CJ, Tuckermann JP, Bauersachs J, Fraccarollo D. The glucocorticoid receptor in monocyte-derived macrophages is critical for cardiac infarct repair and remodeling. *FASEB J* 2017;**31**:5122–5132.

30. Thackeray JT, Hupe HC, Wang Y, Bankstahl JP, Berding G, Ross TL, Bauersachs J, Wollert KC, Bengel FM. Myocardial inflammation predicts remodeling and neuroinflammation after myocardial infarction. *J Am Coll Cardiol* 2018;**71**:263–275.

31. Thackeray JT, Derlin T, Haghikia A, Napp LC, Wang Y, Ross TL, Schafer A, Tillmanns J, Wester HJ, Wollert KC, Bauersachs J, Bengel FM. Molecular imaging of the chemokine receptor CXCR4 after acute myocardial infarction. *JACC Cardiovasc Imaging* 2015;**8**:1417–1426.

32. van den Borne SW, van de Schans VA, Strzelecka AE, Vervoort-Peters HT, Lijnen PM, Cleutjens JP, Smits JF, Daemen MJ, Janssen BJ, Blankesteijn WM. Mouse strain determines the outcome of wound healing after myocardial infarction. *Cardiovasc Res* 2009;**84**:273–282.

33. Fraccarollo D, Thomas S, Scholz CJ, Hilfiker-Kleiner D, Galuppo P, Bauersachs J. Macrophage mineralocorticoid receptor is a pleiotropic modulator of myocardial infarct healing. *Hypertension* 2019;**73**:102–111.

34. Pfeffer MA, Pfeffer JM, Fishbein MC, Fletcher PJ, Spadaro J, Kloner RA, Braunwald E. Myocardial infarct size and ventricular function in rats. *Circ Res* 1979;**44**:503–512.

35. Fraccarollo D, Galuppo P, Motschenbacher S, Ruetten H, Schafer A, Bauersachs J. Soluble guanylyl cyclase activation improves progressive cardiac remodeling and failure after myocardial infarction. Cardioprotection over ACE inhibition. *Basic Res Cardiol* 2014;**109**:421.

36. Fraccarollo D, Widder JD, Galuppo P, Thum T, Tsikas D, Hoffmann M, Ruetten H, Ertl G, Bauersachs J. Improvement in left ventricular remodeling by the endothelial nitric oxide synthase enhancer AVE9488 after experimental myocardial infarction. *Circulation* 2008;**118**:818–827.

37. Fraccarollo D, Galuppo P, Schraut S, Kneitz S, van Rooijen N, Ertl G, Bauersachs J. Immediate mineralocorticoid receptor blockade improves myocardial infarct healing by modulation of the inflammatory response. *Hypertension* 2008;**51**:905–914.

38. Thum T, Fraccarollo D, Galuppo P, Tsikas D, Frantz S, Ertl G, Bauersachs J. Bone marrow molecular alterations after myocardial infarction: impact on endothelial progenitor cells. *Cardiovasc Res* 2006;**70**:50–60.

39. Pfeffer JM, Pfeffer MA, Braunwald E. Influence of chronic captopril therapy on the infarcted left ventricle of the rat. *Circ Res* 1985;**57**:84–95.

40. Pfeffer MA, Pfeffer JM, Steinberg C, Finn P. Survival after an experimental myocardial infarction: beneficial effects of long-term therapy with captopril. *Circulation* 1985;**72**:406–412.

41. Lindsey ML, Bolli R, Canty JM Jr, Du XJ, Frangogiannis NG, Frantz S, Gourdie RG, Holmes JW, Jones SP, Kloner RA, Lefer DJ, Liao R, Murphy E, Ping P, Przyklenk K, Recchia FA, Schwartz Longacre L, Ripplinger CM, Van Eyk JE, Heusch G. Guidelines for experimental models of myocardial ischemia and infarction. *Am J Physiol Heart Circ Physiol* 2018;**314**:H812–H838.

42. Michael LH, Entman ML, Hartley CJ, Youker KA, Zhu J, Hall SR, Hawkins HK, Berens K, Ballantyne CM. Myocardial ischemia and reperfusion: a murine model. *Am J Physiol* 1995;**269**:H2147–H2154.

43. Korf-Klingebiel M, Reboll MR, Klede S, Brod T, Pich A, Polten F, Napp LC, Bauersachs J, Ganser A, Brinkmann E, Reimann I, Kempf T, Niessen HW, Mizrahi J, Schonfeld HJ, Iglesias A, Bobadilla M, Wang Y, Wollert KC. Myeloid-derived growth factor (C19orf10) mediates cardiac repair following myocardial infarction. *Nat Med* 2015;**21**:140–149.

44. Yeang C, Hasanally D, Que X, Hung MY, Stamenkovic A, Chan D, Chaudhary R, Margulets V, Edel AL, Hoshijima M, Gu Y, Bradford W, Dalton N, Miu P, Cheung DY, Jassal DS, Pierce GN, Peterson KL, Kirshenbaum LA, Witztum JL, Tsimikas S, Ravandi A. Reduction of myocardial ischaemia-reperfusion injury by inactivating oxidized phospholipids. *Cardiovasc Res* 2019;**115**:179–189.

45. Poncelas M, Inserte J, Aluja D, Hernando V, Vilardosa U, Garcia-Dorado D. Delayed, oral pharmacological inhibition of calpains attenuates adverse post-infarction remodelling. *Cardiovasc Res* 2017;**113**:950–961.

46. Porrello ER, Mahmoud AI, Simpson E, Johnson BA, Grinsfelder D, Canseco D, Mammen PP, Rothermel BA, Olson EN, Sadek HA. Regulation of neonatal and adult mammalian heart regeneration by the miR-15 family. *Proc Natl Acad Sci USA* 2013;**110**:187–192.

47. Weinheimer CJ, Lai L, Kelly DP, Kovacs A. Novel mouse model of left ventricular pressure overload and infarction causing predictable ventricular remodelling and progression to heart failure. *Clin Exp Pharmacol Physiol* 2015;**42**:33–40.

48. Nolan SE, Mannisi JA, Bush DE, Healy B, Weisman HF. Increased afterload aggravates infarct expansion after acute myocardial infarction. *J Am Coll Cardiol* 1988;**12**:1318–1325.

49. Linz W, Wiemer G, Schmidts HL, Ulmer W, Ruppert D, Scholkens BA. ACE inhibition decreases postoperative mortality in rats with left ventricular hypertrophy and myocardial infarction. *Clin Exp Hypertens* 1996;**18**:691–712.

50. Kapur NK, Paruchuri V, Aronovitz MJ, Qiao X, Mackey EE, Daly GH, Ughreja K, Levine J, Blanton R, Hill NS, Karas RH. Biventricular remodeling in murine models of right ventricular pressure overload. *PLoS One* 2013;**8**:e70802.

51. Urashima T, Zhao M, Wagner R, Fajardo G, Farahani S, Quertermous T, Bernstein D. Molecular and physiological characterization of RV remodeling in a murine model of pulmonary stenosis. *Am J Physiol Heart Circ Physiol* 2008;**295**:H1351–H1368.

52. Boehm M, Lawrie A, Wilhelm J, Ghofrani HA, Grimminger F, Weissmann N, Seeger W, Schermuly RT, Kojonazarov B. Maintained right ventricular pressure overload induces ventricular-arterial decoupling in mice. *Exp Physiol* 2017;**102**:180–189.

53. Julian FJ, Morgan DL, Moss RL, Gonzalez M, Dwivedi P. Myocyte growth without physiological impairment in gradually induced rat cardiac hypertrophy. *Circ Res* 1981;**49**:1300–1310.

54. Liu Z, Hilbelink DR, Crockett WB, Gerdes AM. Regional changes in hemodynamics and cardiac myocyte size in rats with aortocaval fistulas. 1. Developing and established hypertrophy. *Circ Res* 1991;**69**:52–58.

55. Dart CH Jr, Holloszy JO. Hypertrophied non-failing rat heart; partial biochemical characterization. *Circ Res* 1969;**25**:245–253.

56. van der Vijgh WJF, van Velzen D, van der Poort JSE, Schlüper HMM, Mross K, Feijen J, Pinedo HM. Morphometric study of myocardial changes during doxorubicin-induced cardiomyopathy in mice. *Eur J Cancer Clin Oncol* 1988;**24**:1603–1608.

57. Lother A, Bergemann S, Kowalski J, Huck M, Gilsbach R, Bode C, Hein L. Inhibition of the cardiac myocyte mineralocorticoid receptor ameliorates doxorubicin-induced cardiotoxicity. *Cardiovasc Res* 2018;**114**:282–290.

58. Zhu W, Reuter S, Field LJ. Targeted expression of cyclin D2 ameliorates late stage anthracycline cardiotoxicity. *Cardiovasc Res* 2019;**115**:960–965.

59. Hullin R, Metrich M, Sarre A, Basquin D, Maillard M, Regamey J, Martin D. Diverging effects of enalapril or eplerenone in primary prevention against doxorubicin-induced cardiotoxicity. *Cardiovasc Res* 2018;**114**:272–281.

60. Hayward R, Hydock DS. Doxorubicin cardiotoxicity in the rat: an in vivo characterization. *J Am Assoc Lab Anim Sci* 2007;**46**:20–32.

61. Oudit GY, Crackower MA, Eriksson U, Sarao R, Kozieradzki I, Sasaki T, Irie-Sasaki J, Gidrewicz D, Rybin VO, Wada T, Steinberg SF, Backx PH, Penninger JM. Phosphoinositide 3-kinase gamma-deficient mice are protected from isoproterenol-induced heart failure. *Circulation* 2003;**108**:2147–2152.

62. Teerlink JR, Pfeffer JM, Pfeffer MA. Progressive ventricular remodeling in response to diffuse isoproterenol-induced myocardial necrosis in rats. *Circ Res* 1994;**75**:105–113.

63. Werchan PM, Summer WR, Gerdes AM, McDonough KH. Right ventricular performance after monocrotaline-induced pulmonary hypertension. *Am J Physiol* 1989;**256**:H1328–H1336.

64. Angelini A, Castellani C, Virzi GM, Fedrigo M, Thiene G, Valente M, Ronco C, Vescovo G. The role of congestion in cardiorenal syndrome type 2: new pathophysiological insights into an experimental model of heart failure. *Cardiorenal Med* 2016;**6**:61–72.

65. Devi S, Kennedy RH, Joseph L, Shekhawat NS, Melchert RB, Joseph J. Effect of long-term hyperhomocysteinemia on myocardial structure and function in hypertensive rats. *Cardiovasc Pathol* 2006;**15**:75–82.

66. Joseph J, Joseph L, Shekhawat NS, Devi S, Wang J, Melchert RB, Hauer-Jensen M, Kennedy RH. Hyperhomocysteinemia leads to pathological ventricular hypertrophy in normotensive rats. *Am J Physiol Heart Circ Physiol* 2003;**285**:H679–H686.

67. Joseph J, Washington A, Joseph L, Koehler L, Fink LM, Hauer-Jensen M, Kennedy RH. Hyperhomocysteinemia leads to adverse cardiac remodeling in hypertensive rats. *Am J Physiol Heart Circ Physiol* 2002;**283**:H2567–H2574.

68. Capasso JM, Li P, Guideri G, Malhotra A, Cortese R, Anversa P. Myocardial mechanical, biochemical, and structural alterations induced by chronic ethanol ingestion in rats. *Circ Res* 1992;**71**:346–356.

69. Zimmerman MC, Lazartigues E, Sharma RV, Davisson RL. Hypertension caused by angiotensin II infusion involves increased superoxide production in the central nervous system. *Circ Res* 2004;**95**:210–216.

70. Wollert KC, Drexler H. The renin-angiotensin system and experimental heart failure. *Cardiovasc Res* 1999;**43**:838–849.

71. Dahl LK, Heine M, Tassinari L. Role of genetic factors in susceptibility to experimental hypertension due to chronic excess salt ingestion. *Nature* 1962;**194**:480–482.

72. Inoko M, Kihara Y, Morii I, Fujiwara H, Sasayama S. Transition from compensatory hypertrophy to dilated, failing left ventricles in Dahl salt-sensitive rats. *Am J Physiol* 1994;**267**:H2471–H2482.

73. Okamoto K, Aoki K. Development of a strain of spontaneously hypertensive rats. *Jpn Circ J* 1963;**27**:282–293.

74. Yoshioka M, Kayo T, Ikeda T, Koizumi A. A novel locus, Mody4, distal to D7Mit189 on chromosome 7 determines early-onset NIDDM in nonobese C57BL/6 (Akita) mutant mice. *Diabetes* 1997;**46**:887–894.

75. Chavali V, Tyagi SC, Mishra PK. Differential expression of dicer, miRNAs, and inflammatory markers in diabetic Ins2+/- Akita hearts. *Cell Biochem Biophys* 2014;**68**:25–35.

76. Basu R, Oudit GY, Wang X, Zhang L, Ussher JR, Lopaschuk GD, Kassiri Z. Type 1 diabetic cardiomyopathy in the Akita (Ins2WT/C96Y) mouse model is characterized by lipotoxicity and diastolic dysfunction with preserved systolic function. *Am J Physiol Heart Circ Physiol* 2009;**297**:H2096–H2108.

77. Friedman JM, Halaas JL. Leptin and the regulation of body weight in mammals. *Nature* 1998;**395**:763–770.

78. Christoffersen C, Bollano E, Lindegaard ML, Bartels ED, Goetze JP, Andersen CB, Nielsen LB. Cardiac lipid accumulation associated with diastolic dysfunction in obese mice. *Endocrinology* 2003;**144**:3483–3490.

79. Chen H, Charlat O, Tartaglia LA, Woolf EA, Weng X, Ellis SJ, Lakey ND, Culpepper J, Moore KJ, Breitbart RE, Duyk GM, Tepper RI, Morgenstern JP. Evidence that the diabetes gene encodes the leptin receptor: identification of a mutation in the leptin receptor gene in db/db mice. *Cell* 1996;**84**:491–495.

80. Nielsen JM, Kristiansen SB, Norregaard R, Andersen CL, Denner L, Nielsen TT, Flyvbjerg A, Botker HE. Blockage of receptor for advanced glycation end products prevents development of cardiac dysfunction in db/db type 2 diabetic mice. *Eur J Heart Fail* 2009;**11**:638–647.

81. Phillips MS, Liu Q, Hammond HA, Dugan V, Hey PJ, Caskey CJ, Hess JF. Leptin receptor missense mutation in the fatty Zucker rat. *Nat Genet* 1996;**13**:18–19.

82. Clark JB, Palmer CJ, Shaw WN. The diabetic Zucker fatty rat. *Proc Soc Exp Biol Med* 1983;**173**:68–75.

83. Melleby AO, Romaine A, Aronsen JM, Veras I, Zhang L, Sjaastad I, Lunde IG, Christensen G. A novel method for high precision aortic constriction that allows for generation of specific cardiac phenotypes in mice. *Cardiovasc Res* 2018;**114**:1680–1690.

84. Nickel AG, von Hardenberg A, Hohl M, Loffler JR, Kohlhaas M, Becker J, Reil JC, Kazakov A, Bonnekoh J, Stadelmaier M, Puhl SL, Wagner M, Bogeski I, Cortassa S, Kappl R, Pasieka B, Lafontaine M, Lancaster CR, Blacker TS, Hall AR, Duchen MR, Kastner L, Lipp P, Zeller T, Muller C, Knopp A, Laufs U, Bohm M, Hoth M, Maack C. Reversal of mitochondrial transhydrogenase causes oxidative stress in heart failure. *Cell Metab* 2015;**22**:472–484.

85. Koentges C, Pepin ME, Musse C, Pfeil K, Alvarez SVV, Hoppe N, Hoffmann MM, Odening KE, Sossalla S, Zirlik A, Hein L, Bode C, Wende AR, Bugger H. Gene expression analysis to identify mechanisms underlying heart failure susceptibility in mice and humans. *Basic Res Cardiol* 2018;**113**:8.

86. Garcia-Menendez L, Karamanlidis G, Kolwicz S, Tian R. Substrain specific response to cardiac pressure overload in C57BL/6 mice. *Am J Physiol Heart Circ Physiol* 2013;**305**:H397–H402.

87. Cantor EJ, Babick AP, Vasanji Z, Dhalla NS, Netticadan T. A comparative serial echocardiographic analysis of cardiac structure and function in rats subjected to pressure or volume overload. *J Mol Cell Cardiol* 2005;**38**:777–786.

88. Fraccarollo D, Galuppo P, Bauersachs J. Novel therapeutic approaches to post-infarction remodelling. *Cardiovasc Res* 2012;**94**:293–303.

89. Pfeffer MA, Braunwald E, Moyé LA, Basta L, Brown EJ, Cuddy TE, Davis BR, Geltman EM, Goldman S, Flaker GC, Klein M, Lamas GA, Packer M, Rouleau J, Rouleau JL, Rutherford J, Wertheimer JH, Hawkins CM; The SAVE Investigators. Effect of captopril on mortality and morbidity in patients with left ventricular dysfunction after myocardial infarction. Results of the survival and ventricular enlargement trial. *N Engl J Med* 1992;**327**:669–677.

90. Hausenloy DJ, Chilian W, Crea F, Davidson SM, Ferdinandy P, Garcia-Dorado D, van Royen N, Schulz R, Heusch G. The coronary circulation in acute myocardial ischaemia/reperfusion injury—a target for cardioprotection. *Cardiovasc Res* 2019;**115**:1143–1155.

91. Weinheimer CJ, Kovacs A, Evans S, Matkovich SJ, Barger PM, Mann DL. Load-dependent changes in left ventricular structure and function in a pathophysiologically relevant murine model of reversible heart failure. *Circ Heart Fail* 2018;**11**:e004351.

92. Bristow MR, Sageman WS, Scott RH, Billingham ME, Bowden RE, Kernoff RS, Snidow GH, Daniels JR. Acute and chronic cardiovascular effects of doxorubicin in the dog: the cardiovascular pharmacology of drug-induced histamine release. *J Cardiovasc Pharmacol* 1980;**2**:487–515.

93. Lee V, Randhawa AK, Singal PK. Adriamycin-induced myocardial dysfunction *in vitro* is mediated by free radicals. *Am J Physiol* 1991;**261**:H989–H995.

94. Gorini S, De Angelis A, Berrino L, Malara N, Rosano G, Ferraro E. Chemotherapeutic drugs and mitochondrial dysfunction: focus on doxorubicin, trastuzumab, and sunitinib. *Oxid Med Cell Longev* 2018;**2018**:1.

95. Matsumura N, Zordoky BN, Robertson IM, Hamza SM, Parajuli N, Soltys CM, Beker DL, Grant MK, Razzoli M, Bartolomucci A, Dyck J. Co-administration of resveratrol with doxorubicin in young mice attenuates detrimental late-occurring cardiovascular changes. *Cardiovasc Res* 2018;**114**:1350–1359.

96. Thackeray JT, Pietzsch S, Stapel B, Ricke-Hoch M, Lee CW, Bankstahl JP, Scherr M, Heineke J, Scharf G, Haghikia A, Bengel FM, Hilfiker-Kleiner D. Insulin supplementation attenuates cancer-induced cardiomyopathy and slows tumor disease progression. *JCI Insight* 2017;**2**. pii:93098.

97. Meijers WC, Maglione M, Bakker SJL, Oberhuber R, Kieneker LM, de Jong S, Haubner BJ, Nagengast WB, Lyon AR, van der Vegt B, van Veldhuisen DJ, Westenbrink BD, van der Meer P, Silljé HHW, de Boer RA. Heart failure stimulates tumor growth by circulating factors. *Circulation* 2018;**138**:678–691.

98. Engelhardt S, Hein L, Wiesmann F, Lohse MJ. Progressive hypertrophy and heart failure in beta1-adrenergic receptor transgenic mice. *Proc Natl Acad Sci USA* 1999;**96**:7059–7064.

99. Wilson DW, Segall HJ, Pan LC, Lame MW, Estep JE, Morin D. Mechanisms and pathology of monocrotaline pulmonary toxicity. *Crit Rev Toxicol* 1992;**22**:307–325.

100. Sundstrom J, Vasan RS. Homocysteine and heart failure: a review of investigations from the Framingham Heart Study. *Clin Chem Lab Med* 2005;**43**:987–992.

101. Rubin E. Alcoholic myopathy in heart and skeletal muscle. *N Engl J Med* 1979;**301**:28–33.

102. Riehle C, Abel ED. Insulin signaling and heart failure. *Circ Res* 2016;**118**:1151–1169.

103. Gomes AC, Falcão-Pires I, Pires AL, Brás-Silva C, Leite-Moreira AF. Rodent models of heart failure: an updated review. *Heart Fail Rev* 2013;**18**:219–249.

104. Lampreht Tratar U, Horvat S, Cemazar M. Transgenic mouse models in cancer research. *Front Oncol* 2018;**8**:268.

105. Pacak CA, Sakai Y, Thattaliyath BD, Mah CS, Byrne BJ. Tissue specific promoters improve specificity of AAV9 mediated transgene expression following intra-vascular gene delivery in neonatal mice. *Genet Vaccines Ther* 2008;**6**:13.

106. Hintze KJ, Benninghoff AD, Cho CE, Ward RE. Modeling the western diet for preclinical investigations. *Adv Nutr* 2018;**9**:263–271.

107. Takeda T, Hosokawa M, Higuchi K, Hosono M, Akiguchi I, Katoh H. A novel murine model of aging, Senescence-Accelerated Mouse (SAM). *Arch Gerontol Geriatr* 1994;**19**:185–192.

108. Gevaert AB, Shakeri H, Leloup AJ, Van Hove CE, Meyer Gry D, Vrints CJ, Lemmens K, Van Craenenbroeck EM. Endothelial senescence contributes to heart failure with preserved ejection fraction in an aging mouse model. *Circ Heart Fail* 2017;**10**. pii:e003806.

109. Reed AL, Tanaka A, Sorescu D, Liu H, Jeong EM, Sturdy M, Walp ER, Dudley SC Jr, Sutliff RL. Diastolic dysfunction is associated with cardiac fibrosis in the senescence-accelerated mouse. *Am J Physiol Heart Circ Physiol* 2011;**301**:H824–H831.

110. Yue Y, Ghosh A, Long C, Bostick B, Smith BF, Kornegay JN, Duan D. A single intravenous injection of adeno-associated virus serotype-9 leads to whole body skeletal muscle transduction in dogs. *Mol Ther* 2008;**16**:1944–1952.

111. Huang WY, Aramburu J, Douglas PS, Izumo S. Transgenic expression of green fluorescence protein can cause dilated cardiomyopathy. *Nat Med* 2000;**6**:482–483.

112. Hasenfuss G. Animal models of human cardiovascular disease, heart failure and hypertrophy. *Cardiovasc Res* 1998;**39**:60–76.

113. Dobson GP. On being the right size: heart design, mitochondrial efficiency and lifespan potential. *Clin Exp Pharmacol Physiol* 2003;**30**:590–597.

114. Milani-Nejad N, Janssen PM. Small and large animal models in cardiac contraction research: advantages and disadvantages. *Pharmacol Ther* 2014;**141**:235–249.

115. Haghighi K, Kolokathis F, Pater L, Lynch RA, Asahi M, Gramolini AO, Fan GC, Tsiapras D, Hahn HS, Adamopoulos S, Liggett SB, Dorn GW 2nd, MacLennan DH, Kremastinos DT, Kranias EG. Human phospholamban null results in lethal dilated cardiomyopathy revealing a critical difference between mouse and human. *J Clin Invest* 2003;**111**:869–876.

116. Riehle C, Bauersachs J. Key inflammatory mechanisms underlying heart failure. *Herz* 2019;**44**:96.

117. Takimoto E, Champion HC, Li M, Belardi D, Ren S, Rodriguez ER, Bedja D, Gabrielson KL, Wang Y, Kass DA. Chronic inhibition of cyclic GMP phosphodiesterase 5A prevents and reverses cardiac hypertrophy. *Nat Med* 2005;**11**:214–222.

118. Redfield MM, Chen HH, Borlaug BA, Semigran MJ, Lee KL, Lewis G, LeWinter MM, Rouleau JL, Bull DA, Mann DL, Deswal A, Stevenson LW, Givertz MM, Ofili EO, O'Connor CM, Felker GM, Goldsmith SR, Bart BA, McNulty SE, Ibarra JC, Lin G, Oh JK, Patel MR, Kim RJ, Tracy RP, Velazquez EJ, Anstrom KJ, Hernandez AF, Mascette AM, Braunwald E; . RELAX Trial. Effect of phosphodiesterase-5 inhibition on exercise capacity and clinical status in heart failure with preserved ejection fraction: a randomized clinical trial. *JAMA* 2013;**309**:1268–1277.

119. Samuel CS, Cendrawan S, Gao XM, Ming Z, Zhao C, Kiriazis H, Xu Q, Tregear GW, Bathgate RA, Du XJ. Relaxin remodels fibrotic healing following myocardial infarction. *Lab Invest* 2011;**91**:675–690.

120. Teerlink JR, Voors AA, Ponikowski P, Pang PS, Greenberg BH, Filippatos G, Felker GM, Davison BA, Cotter G, Gimpelewicz C, Boer-Martins L, Wernsing M, Hua TA, Severin T, Metra M. Serelaxin in addition to standard therapy in acute heart failure: rationale and design of the RELAX-AHF-2 study. *Eur J Heart Fail* 2017;**19**:800–809.